

Electron correlation in two-electron atoms: A Bohmian analysis of high-order harmonic generation in high-frequency domain

Yang Song(宋阳), Shu Han(韩姝), Yujun Yang(杨玉军), and Fuming Guo(郭福明)

Citation: Chin. Phys. B, 2024, 33 (**12**): 123201. DOI: 10.1088/1674-1056/ad84d1
Journal homepage: http://cpb.iphy.ac.cn; http://iopscience.iop.org/cpb

What follows is a list of articles you may be interested in

Interference of harmonics emitted by different tunneling momentum channels in laser fields

Ling-Yu Zhang(张玲玉), Zhuo-Xuan Xie(谢卓璇), Can Wang(王灿), Xin-Lei Ge(葛鑫磊), and Jing Guo(郭静)
Chin. Phys. B, 2024, 33 (**9**): 093201. DOI: 10.1088/1674-1056/ad5d95

Ionization of two-electron atom (xenon) studied by Bohmian mechanics theory

Yang Song(宋阳), Shu Han(韩姝), Yu-Jun Yang(杨玉军), Fu-Ming Guo(郭福明), and Su-Yu Li(李苏宇)
Chin. Phys. B, 2020, 29 (**11**): 113201. DOI: 10.1088/1674-1056/abb22e

Resonance-enhanced two-photon ionization of hydrogen atom in intense laser field investigated by Bohmian-mechanics

Yang Song(宋阳), Shu Han(韩姝), Yu-Jun Yang(杨玉军), Fu-Ming Guo(郭福明), Su-Yu Li(李苏宇)
Chin. Phys. B, 2020, 29 (**9**): 093204. DOI: 10.1088/1674-1056/aba09e

High-order harmonic generation in a two-color strong laser field with Bohmian trajectory theory

Yi-Yi Huang(黄祎祎), Xuan-Yang Lai(赖炫扬), Xiao-Jun Liu(柳晓军)
Chin. Phys. B, 2018, 27 (**7**): 073204. DOI: 10.1088/1674-1056/27/7/073204

Electron excitation from ground state to first excited state: Bohmian mechanics method

Yang Song(宋阳), Shuang Zhao(赵双), Fu-Ming Guo(郭福明), Yu-Jun Yang(杨玉军), Su-Yu Li(李苏宇)
Chin. Phys. B, 2016, 25 (**3**): 033204. DOI: 10.1088/1674-1056/25/3/033204

Electron correlation in two-electron atoms: A Bohmian analysis of high-order harmonic generation in high-frequency domain

Yang Song(宋阳)[1], Shu Han(韩姝)[2], Yujun Yang(杨玉军)[3,†], and Fuming Guo(郭福明)[3,‡]

[1] *College of Science, Northeast Electric Power University, Jilin* 132012, *China*
[2] *Archives, Northeast Electric Power University, Jilin* 132012, *China*
[3] *Institute of Atomic and Molecular Physics, Jilin University, Changchun* 130012, *China*

(Received 22 August 2024; revised manuscript received 26 September 2024; accepted manuscript online 9 October 2024)

In studying interactions between intense laser fields and atoms or molecules, the role of electron correlation effects on the dynamical response is an important and pressing issue to address. Utilizing Bohmian mechanics (BM), we have theoretically explored the two-electron correlation characteristics while generating high-order harmonics in xenon atoms subjected to intense laser fields. We initially employed Bohmian trajectories to reproduce the dynamics of the electrons and subsequently utilized time-frequency analysis spectra to ascertain the emission time windows for high-order harmonics. Within these time windows, we classified the nuclear region Bohmian trajectories and observed that intense high-order harmonics are solely generated when paired Bohmian particles (BPs) concurrently appear in the nuclear region and reside there for a duration within a re-collision time window. Furthermore, our analysis of characteristic trajectories producing high-order harmonics led us to propose a two-electron re-collision model to elucidate this phenomenon. The study demonstrates that intense high-order harmonics are only generated when both electrons are in the ground state within the re-collision time window. This work discusses the implications of correlation effects between two electrons and offers valuable insights for studying correlation in multi-electron high-order harmonic generation.

Keywords: Bohmian mechanics, high-order harmonics generation, two-electron atom

PACS: 32.80.Rm, 42.50.Hz **DOI:** 10.1088/1674-1056/ad84d1

1. Introduction

With the rapid development of laser technology, laser power has now reached the order of peta-Watts, and the intensity of the laser electric field can be compared to the atomic Coulomb field. Many physical phenomena in strong fields cannot be explained by perturbation theory, including high-order harmonic generation (HHG),[1] above-threshold ionization (ATI),[2,3] and non-sequential double ionization.[4] High-order harmonics are essential for obtaining XUV light and soft x-ray coherent radiation sources,[5] and generating attosecond pulses.[6–8] High-intensity, ultrashort attosecond pulses aid in detecting and manipulating ultrafast processes at the atomic scale, offering a crucial means to understand electronic behavior profoundly.

The theory of high-order harmonic generation primarily encompasses numerical solutions to the time-dependent Schrödinger equation (TDSE),[9–11] the semi-classical "three-step model" approach,[12,13] and the strong field approximation (SFA) method.[14] Among these, the TDSE method is the most accurate; however, for two-electron problems, precise computations in higher dimensions still present challenges. Nonetheless, a one-dimensional (1D) model can still yield results consistent with experiments for linearly polarized laser.[15] Several authors have discussed the high-order harmonic generation process involving double electron effects based on the TDSE method.[16–20] These works suggest that multi-electron effects may produce high-order harmonics. However, based on a probabilistic interpretation, orthodox quantum mechanics cannot track the trajectories of two electrons, making it difficult to ascertain which potential trajectories dominate in generating high-order harmonics. Furthermore, it fails to depict the correlated dynamical processes between the two electrons while producing high-order harmonics. Nevertheless, we can employ BM to trace the trajectories of two electrons and discuss the correlated properties they exhibit during the generation of high-order harmonics.

The BM theory, introduced by Louis de Broglie and further developed by David Bohm, presents an alternative interpretation of quantum mechanics. It suggests that electrons possess specific positions and momentum, making it possible to trace their paths. In this theory, particle movement is guided by the wave function and influenced by a quantum potential, exhibiting non-locality in line with traditional quantum theory. This theory not only reproduces the results of mainstream quantum mechanics flawlessly but also facilitates the straightforward extraction of dynamical information about particles from quantum phenomena.

The BM theory has been widely applied in studying high-power laser interactions with single-electron systems, includ-

†Corresponding author. E-mail: yangyj@jlu.edu.cn
‡Corresponding author. E-mail: guofm@jlu.edu.cn

© 2024 Chinese Physical Society and IOP Publishing Ltd

ing ionization,[21–26] excitation,[27] and high-order harmonic generation processes.[28–31] This framework has been employed in dual-electron systems to investigate the dynamics of ionization processes.[32,33] However, its application to the study of inter-electronic correlation effects in high-order harmonic generation has yet to be widespread and warrants further in-depth exploration. Consequently, this work addresses the issue of electronic correlation in generating high-order harmonics involving two electrons.

2. Theoretical methods

For a two-electron system, under the length gauge and dipole approximation, the time-dependent Schrödinger equation (TDSE) in 1D xenon atoms is given by Eq. (1) (unless otherwise specified, atomic units are used throughout this paper):

$$\mathrm{i}\frac{\partial}{\partial t}\psi(x_1,x_2,t)=\left[-\frac{1}{2}\frac{\partial^2}{\partial x_1^2}-\frac{1}{2}\frac{\partial^2}{\partial x_2^2}+V_a(x_1,x_2)+V_I(x_1,x_2)+(x_1+x_2)E(t)\right]\psi(x_1,x_2,t). \tag{1}$$

In this context,

$$V_a(x_1,x_2)=V_{a1}+V_{a2}=-\frac{2}{\sqrt{x_1^2+4.26}}-\frac{2}{\sqrt{x_2^2+4.26}}$$

represents the Coulomb potential energy between the two electrons and the nucleus, while

$$V_I(x_1,x_2)=\frac{1}{\sqrt{(x_1-x_2)^2+6.5}}$$

represents the Coulomb potential energy between the two electrons.

$$E(t)=E_0\exp\left[-2\log 2\frac{(t-0.35T)^2}{\tau^2}\right]\times\cos[\omega(t-0.35T)+\phi]$$

is a laser electric field, the parameters are as follows: $E_0=0.13$ a.u. (atomic unit), $T=110.23$ a.u., $\tau=31.49$ a.u., $\phi=0.5\pi$, and $\omega=0.057$ a.u. We calculate the ground-state wave function using the imaginary time evolution method. For the numerical solution of Eq. (1), we employ the split-operator technique, which allows us to obtain the wave function at any given time. From the wave function, we can compute the average acceleration of the electron. Taking the first electron as an example:

$$\langle a_1(t)\rangle=\langle\psi(x_1,x_2,t)|-\nabla V_{a1}(x_1)-E(t)|\psi(x_1,x_2,t)\rangle. \tag{2}$$

By performing a Fourier transform on the dipole acceleration, we can obtain the emission power spectrum of the high-order harmonics generated by the first electron:

$$P_1(\Omega)=\left|\frac{1}{t_\mathrm{F}-t_\mathrm{I}}\frac{1}{\Omega^2}\int_{t_\mathrm{I}}^{t_\mathrm{F}}\exp(-\mathrm{i}\Omega t)\langle a_1(t)\rangle\,\mathrm{d}t\right|^2. \tag{3}$$

According to BM theory,[32] we can rewrite the time-dependent two-electron wave function

$$\psi(x_1,x_2,t)=R(x_1,x_2,t)\exp[\mathrm{i}S(x_1,x_2,t)], \tag{4}$$

where R and S are real numbers. Substituting Eq. (4) into Eq. (1), and extracting imaginary and real parts on both sides of the equation, we can obtain the following equations:

$$\frac{\partial R^2(x_1,x_2,t)}{\partial t}+\sum_{i=1}^{2}\frac{\partial}{\partial x_i}\left[\frac{\partial S(x_1,x_2,t)}{\partial x_i}R^2(x_1,x_2,t)\right]=0, \tag{5}$$

$$-\frac{\partial S(x_1,x_2,t)}{\partial t}=\sum_{i=1}^{2}\frac{1}{2}\left[\frac{\partial S(x_1,x_2,t)}{\partial x_i}\right]^2+Q(x_1,x_2,t)+V_a(x_1,x_2)+(x_1+x_2)E(t). \tag{6}$$

Equation (4) is the quantum Hamilton–Jacobian equation, where the subscript i denotes the i-th electron. The expression of quantum potential is

$$Q(x_1,x_2,t)=\sum_{i=1}^{2}-\frac{1}{2}\frac{\partial^2 R(x_1,x_2,t)}{\partial x_i^2}\Big/R(x_1,x_2,t). \tag{7}$$

According to BM, the velocity of the i-th electron can also be expressed by the wave-function

$$v_i(t)=\mathrm{Im}\left[\frac{1}{\psi(x_1,x_2,t)}\frac{\partial}{\partial x_i}\psi(x_1,x_2,t)\right]\Big|_{x_1=x_1(t),x_2=x_2(t)}. \tag{8}$$

Therefore, we can get the position of the i-th electron at any time

$$x_i(t)=x_i(0)+\int_0^t v_i(t')\,\mathrm{d}t'. \tag{9}$$

First, the imaginary time evolution method is used to calculate the probability density function of the ground state of the xenon atom at an initial instant $|\psi_0(x_1,x_2,0)|^2$. The initial spatial positions of N pairs of Bohmian particles (BPs) are then given at random by sampling $|\psi_0(x_1,x_2,0)|^2$ using the acceptance–rejection sampling method and used to denote the possible initial positions of two electrons, i.e., $x_1^k(t=0)$ and $x_2^k(t=0)$ ($k=1,2,3,\ldots,N$ denotes the k-th BP). The second-order symmetric difference method is then used to calculate the time evolution of the wave function $\psi(x_1,x_2,t)$ of a 1D xenon atom in a laser field. The wave-function's initial state follows the spatial exchange symmetry. The multi-body BM is used to determine the velocities and trajectories of paired particles:

$$v_1^k(t)=\frac{\mathrm{d}x_1^k(t)}{\mathrm{d}t}=\mathrm{Im}\left[\frac{1}{\psi(x_1,x_2,t)}\frac{\partial\psi(x_1,x_2,t)}{\partial x_1}\right]\Big|_{x_1=x_1^k(t),x_2=x_2^k(t)}, \tag{10}$$

$$v_2^k(t) = \frac{\mathrm{d}x_2^k(t)}{\mathrm{d}t} = \mathrm{Im}\left[\frac{1}{\psi(x_1,x_2,t)}\frac{\partial\psi(x_1,x_2,t)}{\partial x_2}\right]\Bigg|_{x_1=x_1^k(t),x_2=x_2^k(t)}, \quad (11)$$

$$x_1^k(t) = x_1^k(0) + \int_0^t v_1^k(t')\mathrm{d}t',$$

$$x_2^k(t) = x_2^k(0) + \int_0^t v_2^k(t')\mathrm{d}t'. \quad (12)$$

3. Results and discussion

3.1. Xenon atomic potential model

Initially, we employed 200 Bohmian trajectories to delineate the dynamical process of the first electron. As depicted in Fig. 1(b), under the specific conditions of the laser electric field illustrated, it was observed that the single-electron wave packet, as presented in Eq. (13) and computed using TDSE, aligns closely with the temporal evolution images of the Bohmian trajectories. This congruence suggests that Bohmian trajectories can accurately represent the motion of electron wave packets.

$$|\psi(x_1,t)|^2 = \int_{-\infty}^{+\infty}\psi(x_1,x_2,t)^*\psi(x_1,x_2,t)\mathrm{d}x_2. \quad (13)$$

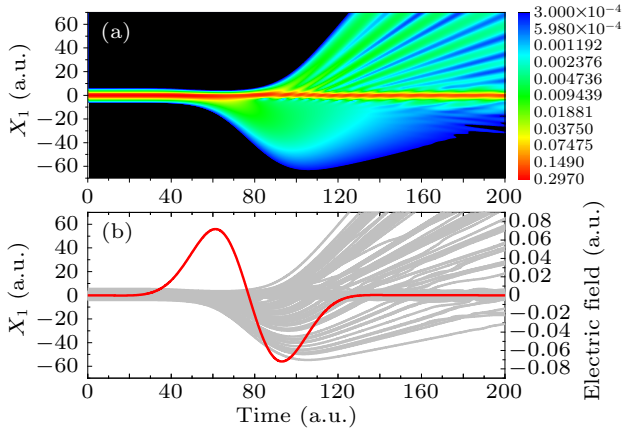


Fig. 1. Time-evolution of the first electron in a laser field with a central frequency of 0.057 a.u. and a duration of 2 optical cycles. (a) Time-evolution of the wave packet obtained from numerical solutions to the TDSE; (b) time-evolution of 200 Bohmian trajectories (gray solid lines) in the presence of the laser electric field (red solid line).

We present the high-order harmonic spectrum and time–frequency analysis of the first electron, as shown in Fig. 2. Through analysis, we find that the cutoff frequency of high-order harmonics is located near $\Omega = 1.1$ a.u. (dashed line), and the occurrence time of high-order harmonics is between 95 a.u.–123 a.u. Next, we will use the Bohmian trajectory to analyze the trajectory characteristics of two electrons within this time window.

We randomly selected 200 pairs of BPs and roughly divided their trajectories into three sets: The first, as shown in Figs. 3(a) and 3(d) are characterized by the paired trajectories being very close to the nucleus and the two particles being close to each other. More notably, the two particles exhibited high-frequency oscillations after approaching each other. This behavior suggests that such trajectories generate intense high-order harmonics.[32] The second set, as depicted in Figs. 3(b) and 3(e) are characterized by the absence of high-frequency oscillations within the time window, indicating a minimal likelihood of generating intense high-order harmonics. Figure 3(b) is because the re-collision particle (black solid line) has returned to the nuclear region after the time window and did not interact with the nuclear region particles (red dashed line) within that time window. In Fig. 3(e), both particles are far from the nuclear region at the start of the time window. The third set, illustrated in Figs. 3(c) and 3(f), features unique trajectories. In Fig. 3(c), one particle remains in the nuclear region while the other leaves near the beginning of the time window. Figure 3(f) illustrates a scenario where one particle undergoes ionization followed by re-collision (represented by the black solid line). However, when this particle is in proximity to its paired particle (indicated by the red dotted line), either the distance between them is large (greater than 5 a.u.), or the duration of their closeness is short (less than one-quarter of the time window). Although some high-frequency oscillations are observed for BPs near the nucleus in Figs. 3(c) and 3(f), these oscillations have small amplitudes, unstable frequencies, and chaotic phases, which could lead to a diminished amplitude in the synthesized vibration, making it difficult to generate intense high-order harmonics.

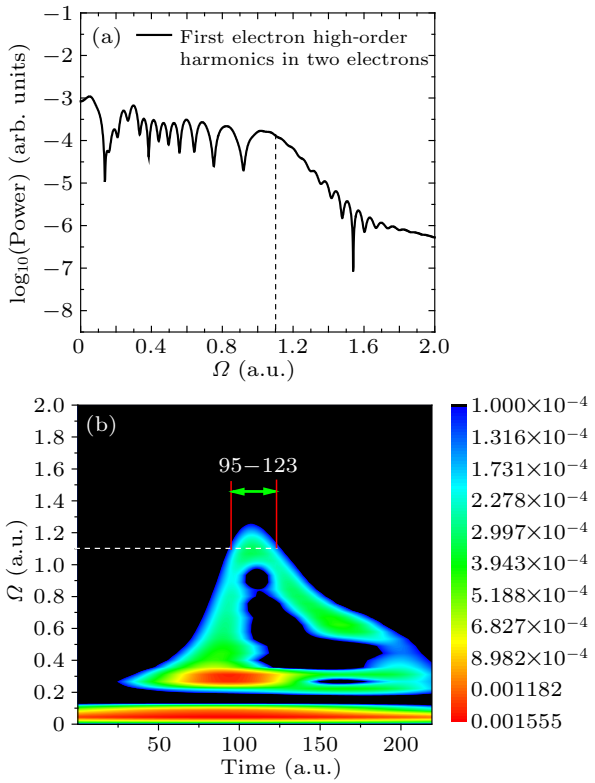


Fig. 2. (a) High-order harmonic spectrum of the first electron calculated using TDSE, (b) time–frequency analysis spectrum of the first electron.

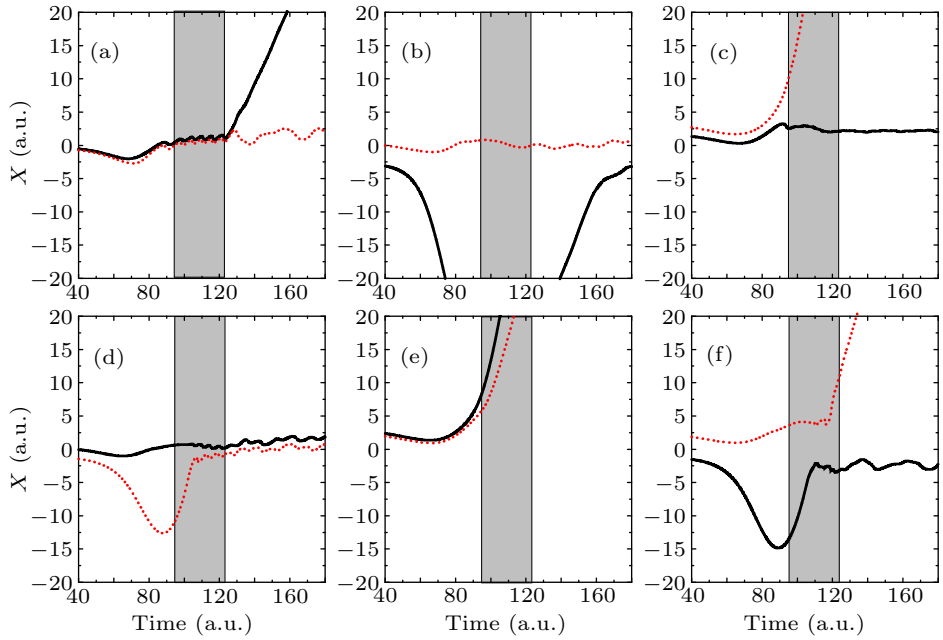


Fig. 3. Illustration of several scenarios of paired trajectories within the time window (a gray area): (a) and (d) both BPs remain close to the nucleus, exhibiting pronounced high-frequency vibrations with stable frequency and phase; (b) and (e) one or both BPs are distant from the nucleus, resulting in fragile vibrational behavior; (c) and (f) one trajectory stays in the nuclear region while the other leaves before the time window, or the two particles are far apart and have a short interaction time, leading to weak vibrations with unstable frequency and phase.

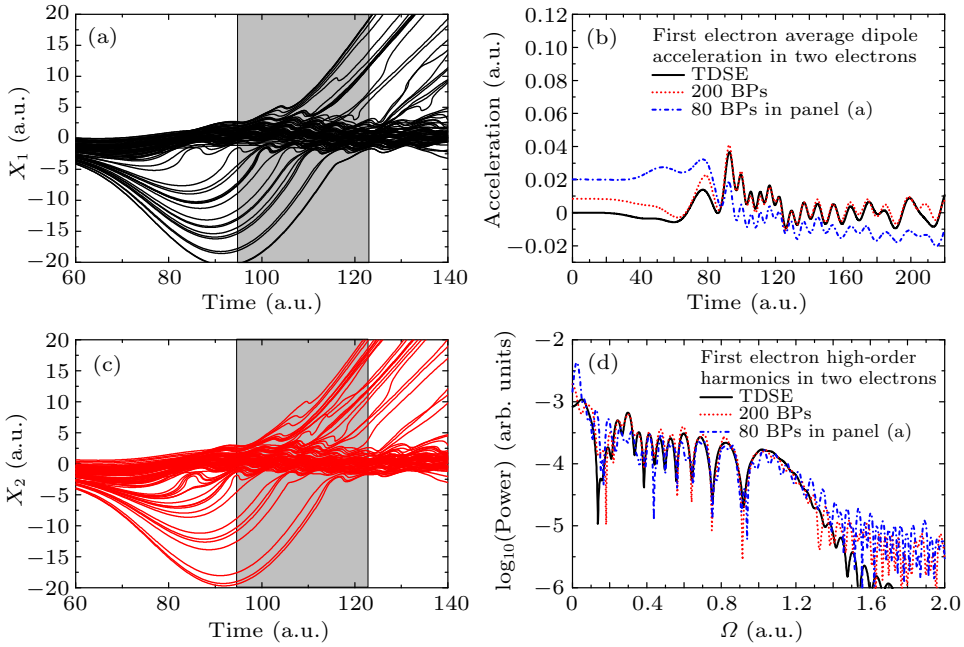


Fig. 4. Trajectories of 80 pairs of BPs generating high-order harmonics: (a) 80 trajectories from the first electron; (c) 80 trajectories from the second electron; (b) dipole acceleration comparison of the first electron, where TDSE (black solid line), 200 BPs (red dotted line), 80 BPs (blue dash-dotted line); (d) high-order harmonic comparison of the first electron, where TDSE (black solid line), 200 BPs (red dotted line), 80 BPs (blue dash-dotted line).

To quantitatively describe the emission of high-order harmonics by BPs in the three trajectory types mentioned above, we classified and statistically analyzed these 200 pairs of BPs based on the characteristics of the three sets of trajectories.

For the first set of statistical methods and results, inspired by the trajectories in Figs. 3(a) and 3(d), the statistical method is as follows: when a pair of BPs stay together for more than one-quarter of the window time, and both the distance between the two BPs and their distances from the nucleus are less than 5 a.u., their trajectories are shown in Figs. 4(a) and 4(b). The black solid line trajectory in Fig. 4(a) originates from the first electron, and the red solid line trajectory in Fig. 4(b) originates from the second electron. From the trajectories, we can observe that the particles exhibit re-collision behavior and significant high-frequency oscillation behavior within the time window, with relatively stable frequencies and phases, suggesting

that these trajectories are highly likely to generate high-order harmonics. The statistical results show that there are 80 such pairs of trajectories. We calculated the average dipole acceleration and high-order harmonics for the 80 BPs from the first electron, as indicated by the blue dotted lines in Figs. 4(b) and 4(d), respectively. We found that the high-order harmonics generated by these 80 trajectories are consistent with those represented by 200 BPs from the first electron and the results from TDSE calculations, indicating that almost all high-order harmonics from the first electron come from these 80 trajectories.

In studying the second set of statistical methods and results, we were inspired by the characteristics of the trajectories in Figs. 3(b) and 3(e) to design the following statistical methods: Firstly, we conducted statistics on particles that undergo re-collision, particularly those whose re-collision time is greater than or equal to the end of the time window ($t = 123$ a.u.). Secondly, we also tallied the trajectories where particles were already far from the core region at the beginning of the time window ($t = 95$ a.u.). Figure 5(a) displays the trajectories from the first electron, while figure 5(c) shows those from the second electron. There are a total of 53 pairs of such trajectories. Due to the absence of re-collision events within the time window(as shown in Figs. 5(a) and 5(c)), the BPs in the nuclear region exhibit no high-frequency oscillations (as shown in Fig. 5(a)). Consequently, no high-order harmonic generation occurs (as shown in Fig. 5(d)).

In the third set of statistical methods and results, we analyzed the trajectories shown in Figs. 3(c) and 3(f). The characteristics of these trajectories are as follows. In Fig. 3(c), one particle of the pair leaves the core region under the influence of the external field while the other remains; in Fig. 3(f), one particle of the pair returns to the core region after ionization in the external field and recombines with the other particle. Although re-collision occurs within the time window, the two particles cannot simultaneously satisfy the conditions of being sufficiently close (less than 5 a.u.) and coexisting for a sufficiently long period (more than 1/4 of the window time). From this, we counted a total of 67 such trajectory pairs. We are observing the trajectories in Figs. 6(a) and 6(c), it can be seen that although the particles within the core region exhibit oscillatory behavior, the amplitude of oscillation for each particle is small, the frequencies are unstable, and the phases are inconsistent, which leads to irregular vibrations of the particles, making it difficult to produce high-order harmonics. We calculated the average dipole acceleration and harmonic spectrum for these 67 BPs originating from the first electron, with the results shown in Figs. 6(c) and 6(d). The findings indicate that no strong high-order harmonics were generated.

From the statistical analysis above, we have discovered that the generation of high-order harmonics requires the following conditions: both particles must be present within the time window; the pair of BPs must be located in the core region simultaneously (less than 5 a.u. from the atomic nucleus); and these two particles must be very close to each other (less than 5 a.u. apart), with this state lasting for a sufficiently long duration (more than 1/4 of the time window).

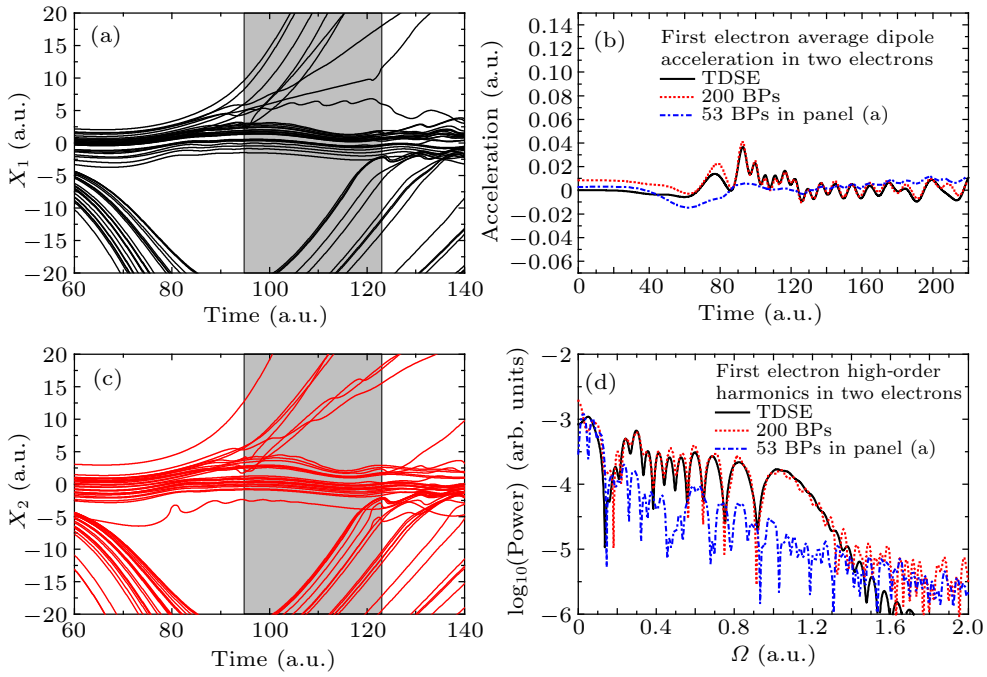


Fig. 5. The trajectories of 53 pairs of BPs that do not produce high-order harmonics: (a) 53 trajectories from the first electron; (c) 53 trajectories from the second electron; (b) dipole acceleration comparison of the first electron, where TDSE (black solid line), 200 BPs (red dotted line), 53 BPs (blue dash-dotted line); (d) high-order harmonic comparison of the first electron, where TDSE (black solid line), 200 BPs (red dotted line), 53 BPs (blue dash-dotted line).

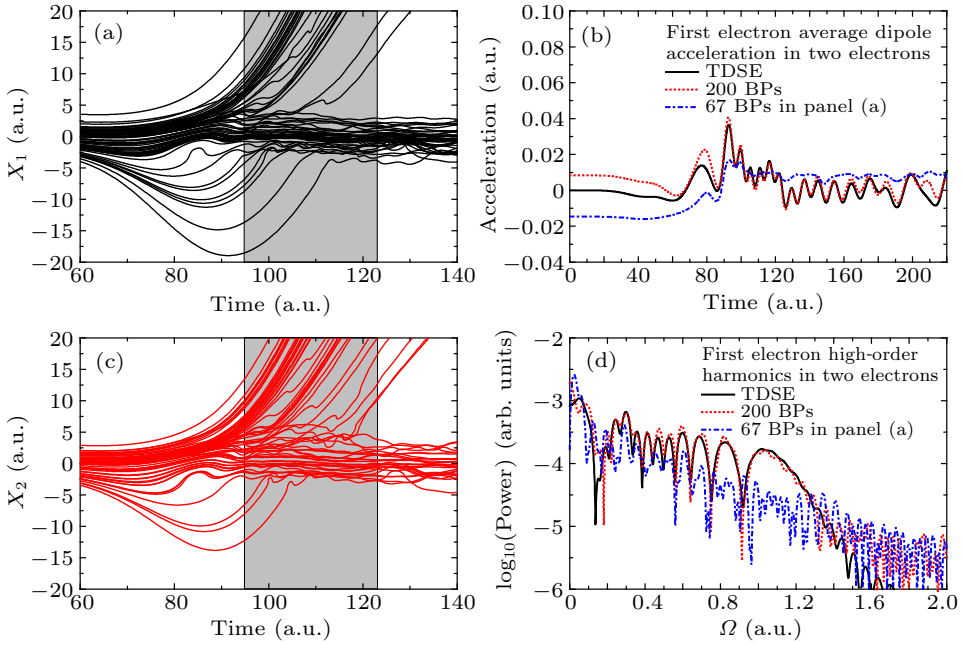


Fig. 6. The trajectories of 67 pairs of BPs that do not produce high-order harmonics: (a) 67 trajectories from the first electron; (c) 67 trajectories from the second electron; (b) dipole acceleration comparison for the first electron, where TDSE (black solid line), 200 BPs (red dotted line), 67 BPs (blue dash-dotted line); (d) high-order harmonic comparison for the first electron, where TDSE (black solid line), 200 BPs (red dotted line), 67 BPs (blue dash-dotted line).

3.2. Two-electron re-collision model

Next, we will explore why, in the first set, the trajectories of 80 BPs almost entirely generated high-order harmonics for the first electron. Through statistical analysis, we have discovered that the production of high-order harmonics requires both particles to be simultaneously located in the core region for an extended period. The wave function describing both particles together in the core region is the ground state wave function $\psi_{\text{ground}}(x_1,x_2,t)$ of the two-electron system. Hence, we hypothesize that generating high-order harmonics invariably involves the two-electron ground state wave function. Furthermore, from Fig. 3(d), we have observed that the re-collision phenomenon occurs between two particles: one particle ionizes under the influence of the electric field. Then, it collides with another Bohmian particle in the core region. Based on this, we also assume that the production of high-order harmonics inevitably involves the re-collision state wave function $\psi_{\text{re-coll}}(x_1,x_2,t)$ of the two particles. We denote by

$$\begin{aligned}\psi_{\text{re-coll}}(x_1,x_2,t) &= \phi_{\text{continuous}}(x_1)\times\phi_{\text{ground}}(x_2)\\ &+\phi_{\text{ground}}(x_1)\times\phi_{\text{continuous}}(x_2),\end{aligned}\quad(14)$$

where the ground state wavefunction $\phi_{\text{ground}}(x)$ of one electron is obtained by numerically solving the single-electron schrödinger equation. We define the wavefunction $\phi_{\text{continuous}}(x)$ for the other electron in a continuum state as follows:

$$\begin{aligned}\phi_{\text{continuous}}(x) &= \exp[-4\log 2\times(x+100)^2/\Lambda_0^2]\\ &\times\exp(\mathrm{i}px).\end{aligned}\quad(15)$$

The re-collision state satisfies exchange symmetry. The single-electron wave packet in the continuum state moves towards the core region with momentum p. It collides with the wave packet of the other electron in the ground state, thereby simulating the re-collision process.

From Figs. 3(a) and 3(d), it can be observed that the initial state for generating high-order harmonics should be a superposition of the two-electron ground state $\psi_{\text{ground}}(x_1,x_2,t)$ and the re-collision state $\psi_{\text{re-coll}}(x_1,x_2,t)$.

$$\begin{aligned}\psi_i(x_1,x_2,t) &= C_1\psi_{\text{ground}}(x_1,x_2,t)+C_2[\phi_{\text{continuous}}(x_1)\\ &\times\phi_{\text{ground}}(x_2)+\phi_{\text{ground}}(x_1)\\ &\times\phi_{\text{continuous}}(x_2)].\end{aligned}\quad(16)$$

In the parameters mentioned above $C_1=0.4$, $C_2=0.3$, $\Lambda_0=40$ a.u., and $p=1$ a.u. Since the orthodox quantum theory cannot provide the trajectory of two-electron re-collision, we use the BM theory to analyze the re-collision processes.

Trajectories were selected from the two-electron ground states $\psi_{\text{ground}}(x_1,x_2,t)$ and the re-collision state $\psi_{\text{re-coll}}(x_1,x_2,t)$, as shown in Fig. 7(a). The dotted lines represent the trajectories from ground state $\psi_{\text{ground}}(x_1,x_2,t)$, while the solid lines denote those from re-collision state $\psi_{\text{re-coll}}(x_1,x_2,t)$. Black denotes the first electron, and red represents the second one. As illustrated, when these particles appear together in the core region, they exhibit vibrational patterns characterized by large amplitudes, high frequencies, and stable phase differences. For this purpose, we calculated the harmonic spectrum of the first electron using Eq. (10), as shown in Fig. 7(b). We observed that, under these condi-

tions, pronounced high-order harmonics were indeed generated, with the frequency centre located near $\omega = 0.933$ a.u. The intensity of high-order harmonics reaches its maximum, and their energy should correspond to the sum of the electron's kinetic energy and the single ionization energy. In our xenon atom model, the single ionization energy is determined to be the difference between the two-electron ground state energy (-1.23 a.u.) and the single-electron ground state energy (-0.78 a.u.), which is 0.45 a.u. Considering the electron's kinetic energy of 0.5 a.u., the maximum energy of the harmonics should therefore be 0.45 a.u.+0.5 a.u. = 0.95 a.u. This result is very close to the maximum harmonic value of 0.933 a.u. displayed in Fig. 7(b). The findings indicate that the superposition of the two-electron ground and re-collision states can produce high-order harmonics.

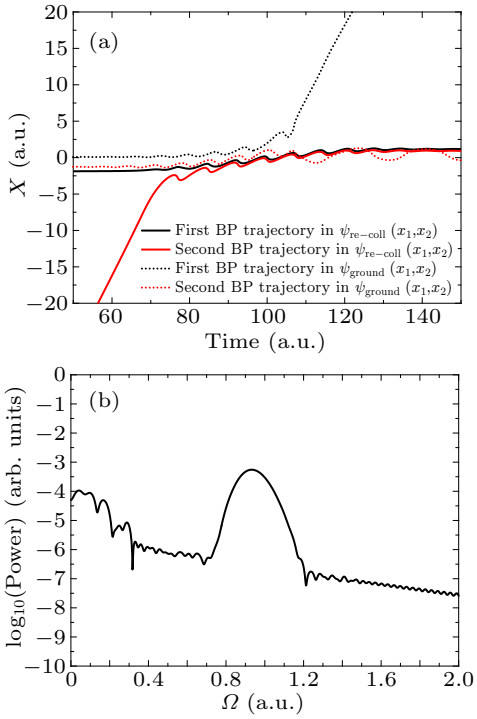


Fig. 7. (a) Bohmian trajectories for $C_1 = 0.4$; the black solid line (red) indicates the Bohmian trajectory of the first (second) electron in state $\psi_{re-coll}(x_1,x_2,t)$, while the black dashed line (red) shows the Bohmian trajectory of the first (second) electron in state $\psi_{ground}(x_1,x_2,t)$. (b) Harmonic spectrum of the first electron calculated by TDSE.

We continue our force analysis on the particle pairs in state $\psi_{re-coll}(x_1,x_2,t)$, as displayed in Fig. 7(a), wherein the black and red solid lines show the trajectories of these particles. Specifically, the force analysis of the black BP is presented in Fig. 8(a), while that of the red BP is shown in Fig. 8(b). The following is the formula for calculating the force exerted on a particle.

The resultant force acting on each BP:

$$F_{\mathrm{R}} = \frac{\mathrm{d}v_i^k(t)}{\mathrm{d}t}.$$

Coulomb force from nucleus acting on the k-th BP of the i-th electron:

$$F_{\text{nucleus Coulomb}} = -\frac{\partial}{\partial x_i}\left[-\frac{2}{\sqrt{(x_i)^2+4.26}}\right]\Bigg|_{x_i=x_i^k(t)}.$$

Coulomb force from the k-th BP of the j-th electron acting on the k-th BP of the i-th electron:

$$F_{\text{e-e Coulomb}} = -\frac{\partial}{\partial x_i}\left[\frac{1}{\sqrt{(x_i-x_j)^2+6.5}}\right]\Bigg|_{x_i=x_i^k(t),x_j=x_j^k(t)}.$$

Quantum force acting on each BP:

$$F_{\mathrm{Q}} = F_{\mathrm{R}} - F_{\text{nucleus Coulomb}} - F_{\text{e-e Coulomb}}.$$

Upon careful examination of Figs. 8(a) and 8(b), it can be discerned that during the recollision process of the particle pair, the two particles are predominantly subjected to quantum forces (QF). While Coulomb repulsion and nuclear attraction exist, they are negligible compared to the QF. The QF, characterized by its high intensity and frequency, effectively binds the particle pair near the nuclear region, thereby facilitating the generation of high-order harmonics, which exhibit significant strength and frequency characteristics.

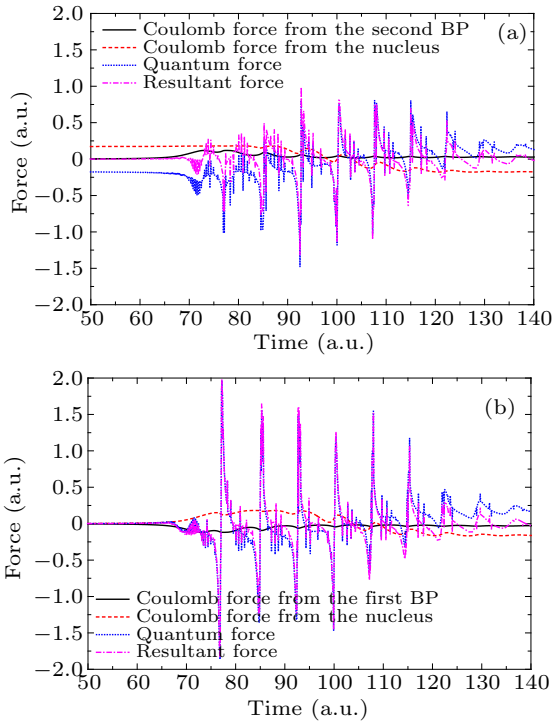


Fig. 8. (a) Resultant force acting on the first BP (short dash-dotted magenta curve) and its component forces, i.e., Coulomb force from the second BP (solid black curve), Coulomb force from the nucleus (short dashed red curve), and quantum force (short dotted blue curve). (b) Resultant force acting on the second BP (short dash-dotted magenta curve) and its component forces, i.e., Coulomb force from the first BP (solid black curve), Coulomb force from the nucleus (short dashed red curve), and quantum force (short dotted blue curve).

In the absence of a two-electron ground state, can high-order harmonics still be generated? To investigate this question, we set $C_1 = 0$ in Eq. (16), thereby reducing the probability of the ground state to zero. Subsequently, we recalculated

the Bohmian trajectories and harmonic spectra, as shown in Figs. 9(a) and 9(b), respectively. Here, both trajectories originate from re-collision state $\psi_{\text{re-coll}}(x_1,x_2,t)$, one from state $\phi_{\text{continuous}}(x)$ and the other from state $\phi_{\text{ground}}(x)$. However, in this scenario, the two-electron ground state $\psi_{\text{ground}}(x_1,x_2,t)$ is absent, with only the re-collision state $\psi_{\text{re-coll}}(x_1,x_2,t)$ present. The trajectories in Fig. 9(a) show that although collisions near the core region occur between the particle pairs, their brief dwell time in this area prevents the generation of high-frequency oscillations. Further examination of the harmonic spectrum under this condition, depicted in Fig. 9(b), reveals that high-order harmonics are not generated. Therefore, we conclude that high-order harmonics cannot be generated in the presence of only the re-collision state $\psi_{\text{re-coll}}(x_1,x_2,t)$ without the ground state $\psi_{\text{ground}}(x_1,x_2,t)$.

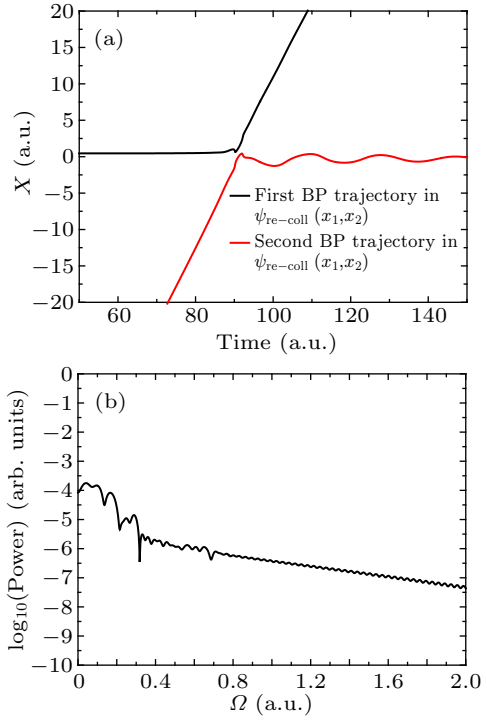


Fig. 9. (a) Bohmian trajectories for $C_1 = 0$; the black solid line (red) indicates the Bohmian trajectory of the first (second) electron in state $\psi_{\text{re-coll}}(x_1,x_2,t)$, while the black dashed line (red) shows the Bohmian trajectory of the first (second) electron in state $\psi_{\text{ground}}(x_1,x_2,t)$. (b) Harmonic spectrum of the first electron calculated by TDSE.

We compared the second set (Figs. 5(a) and 5(c)) and the third set (Figs. 6(a) and 6(c)) of trajectories. The common characteristic of these two trajectories is that, within the observed time window, both electrons did not simultaneously appear in the core region for a sustained period. In other words, the absence of a two-electron ground state during the time window means high-order harmonics could not be generated.

4. Conclusion

We employed the BM approach to numerically solve the time-dependent Schrödinger equation, using xenon atomic potential as the physical model, to investigate the correlated characteristics of high-order harmonic generation by two active electrons: (i) We demonstrated that 200 pairs of BPs could accurately reproduce the dynamics of electrons in an intense laser field. (ii) We utilized the high-order harmonic spectrum and time-frequency analysis of a single electron to determine the emission time window for high-order harmonics. (iii) Within this time window, we analyzed the motion behavior of paired trajectories. We reached a significant conclusion: intense high-order harmonics are only generated when the particle pair must exhibit re-collision behavior; both BPs are simultaneously present in the core region for a duration exceeding approximately one-quarter of the time window.

Using the trajectories mentioned above, we developed a re-collision model to elucidate the reasons behind the harmonic generation. We discovered that intense high-order harmonics are only generated when the two-electron ground state exists during re-collision. This model explains why two BPs must be present in the core region to maintain a sufficiently long coexistence and generate intense high-order harmonics. This paper reveals the simultaneous correlated characteristics of two-electron high-order harmonic emission when both electrons must be in the core region, providing a significant reference value for studying the mechanisms of multi-electron high-order harmonic emission.

Acknowledgement

Project supported by the Natural Science Foundation (General Project) of Jilin Province, China (Grant No. 20230101283JC).

References

[1] Qiao Y, Chen J, Li Z, Liu Y, Jiang S, Liu W, Yang Y and Chen J 2024 *Opt. Lett.* **49** 3986
[2] Chu S I and Cooper J 1985 *Phys. Rev. A* **32** 2769
[3] Javanainen J, Eberly J H and Su Q 1988 *Phys. Rev. A* **38** 3430
[4] Walker B, Sheehy B, DiMauro L F, Agostini P, Schafer K J and Kulander K C 1994 *Phys. Rev. Lett.* **73** 1227
[5] Spielmann Ch, Burnett N H, Sartania S, Koppitsch R, Schnürer M, Kan C, Lenzner M, Wobrauschek P and Krausz F 1997 *Science* **278** 661
[6] Sansone G, Benedetti E, Calegari F, Vozzi C, Avaldi L, Flammini R, Poletto L, Villoresi P, Altucci C, Velotta R, Stagira S, De Silvestri S and Nisoli M 2006 *Science* **314** 443
[7] Corkum P B and Krausz F 2007 *Nat. Phys.* **3** 381
[8] Krausz F and Ivanov M 2009 *Rev. Mod. Phys.* **81** 163
[9] Krause J L, Schafer K J and Kulander K C 1992 *Phys. Rev. Lett.* **68** 3535
[10] Protopapas M, Keitel C H and Knight P L 1997 *Rep. Prog. Phys.* **60** 389
[11] Burnett K, Reed V C and Knight P L 1993 *J. Phys. B* **26** 561
[12] Schafer K J, Yang B, Dimauro L F and Kulander K C 1993 *Phys. Rev. Lett.* **70** 1599
[13] Corkum P B 1993 *Phys. Rev. Lett.* **71** 1994
[14] Lewenstein M, Balcou P, Ivanov M Y, L'Huillier A and Corkum P B 1994 *Phys. Rev. A* **49** 2117
[15] Liu W C, Eberly J H, Haan S L and Grobe R 1999 *Phys. Rev. Lett.* **83** 520
[16] Lappas D G, Sanpera A, Watson J B, Burnett K, Knight P L, Grobe R and Eberly J H 1996 *J. Phys. B* **29** L619

[17] Grobe R and Eberly J H 1993 *Phys. Rev. A* **48** 4664
[18] Koval P, Wilken F, Bauer D and Keitel C H 2007 *Phys. Rev. Lett.* **98** 043904
[19] Bandrauk A D and Lu H Z 2005 *J. Phys. B* **38** 2529
[20] Hu S L and Shi T Y 2013 *Chin. Phys. B* **22** 013101
[21] Lai X Y, Cai Q Y and Zhan M S 2009 *New J. Phys.* **11** 113035
[22] Lai X Y, Cai Q Y and Zhan M S. 2009 *Eur. Phys. J. D* **53** 393
[23] Takemoto N and Becker A 2011 *J. Chem. Phys.* **134** 074309
[24] Wei S S, Li S Y, Guo F M, Yang Y J and Wang B B 2013 *Phys. Rev. A* **87** 063418
[25] Song Y, Yang Y J, Guo F M and Li S Y 2017 *J. Phys. B* **50** 095003
[26] Bohm D 1952 *Phys. Rev.* **85** 166
[27] Song Y, Zhao S, Guo F M, Yang Y J and Li S Y 2016 *Chin. Phys. B* **25** 033204
[28] Lai X Y, Cai Q Y and Zhan M S 2010 *Chin. Phys. B* **19** 020302
[29] Song Y, Guo F M, Li S Y, Chen J G, Zeng S L and Yang Y J 2012 *Phys. Rev. A* **86** 033424
[30] Wu J, Augstein B B and Figueira de Morisson Faria C 2013 *Phys. Rev. A* **88** 023415
[31] Song Y, Li S Y, Liu X S, Guo F M and Yang Y J 2013 *Phys. Rev. A* **88** 053419
[32] Song Y, Han S, Yang Y J, Guo F M and Li S Y 2020 *Chin. Phys. B* **29** 113201
[33] Sawada R, Sato T and Ishikawa K L 2014 *Phys. Rev. A* **90** 023404
[34] Dieter U and Ahrens J H 1974 *Acceptance-Rejection Techniques for Sampling from the Gamma and Beta Distributions* (Stanford, CA: Stanford University Press)